Journal of Hazardous Materials 438 (2022) 129443

Contents lists available at ScienceDirect

Journal of Hazardous Materials

journal homepage: www.elsevier.com/locate/jhazmat

Mice brain metabolomics after the exposure to a "chemical cocktail" and selenium supplementation through the gut-brain axis

C. Parra-Martínez [a], M. Selma-Royo [b], B. Callejón-Leblic [a], M.C. Collado [b,1], N. Abril [c,1], T. García-Barrera [a,1,*]

[a] Research Center of Natural Resources, Health and the Environment (RENSMA). Department of Chemistry, Faculty of Experimental Sciences, University of Huelva, Fuerzas Armadas Ave., 21007 Huelva, Spain
[b] Institute of Agrochemistry and Food Technology (IATA-CSIC), Department of Biotechnology, Agustin Escardino 7, 46980 Paterna, Valencia, Spain
[c] Department of Biochemistry and Molecular Biology, University of Córdoba, Campus de Rabanales, Edificio Severo Ochoa, E-14071 Córdoba, Spain

HIGHLIGHTS

- "Chemical cocktails" altered mainly mice brain lipids and aminoacids pathways.
- Se intake, gut microbiota and brain metabolites interact affecting host health.
- Several gut microbes are associated with specific brain metabolites.
- Selenium antagonized several brain metabolites impaired by the "chemical cocktail".

GRAPHICAL ABSTRACT

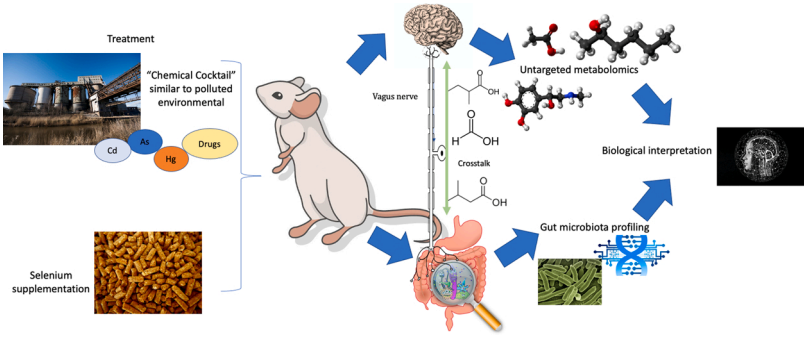

ARTICLE INFO

Editor: Jörg Rinklebe

Keywords:
Brain metabolomics
Selenium
Chemical cocktails

ABSTRACT

Several environmental pollutants have been shown to damage brain and affect gut microbiota. Limited evidence is available about the impact of "chemical cocktails" (CC) of xenobiotics on brain metabolome and their possible influence in the gut-brain crosstalk. To this end, BALB/c mice were exposed to heavy metals (As, Hg, Cd) and pharmaceuticals (diclofenac and flumequine) under regular rodent diet or supplemented with selenium (Se). Selenium, an antioxidant well-known for its antagonism against the neurotoxicity of several pollutants,

Abbreviations: C, control mice group fed rodent diet; CC, mice fed regular diet exposed to the chemical cocktail; CC-Se, mice fed Se supplemented diet exposed to the chemical cocktail; CC-Abx, antibiotic treated-mice fed regular diet exposed to the chemical cocktail; CC-Abx-Se, Antibiotic treated-mice fed Se supplemented diet exposed to the chemical cocktail; KRI, Kovaťs retention indexes; FC, Fold change; PE, phosphatidylethanolamine; PC, phosphatidylcholine; PS, phosphatidylserine; cer, ceramide; PI, phosphatidylinositol; GPCh, glycerophosphocholine: PCh, phosphocholine; Ch, choline; BMI, body mass index; AN, anorexia nervosa; QC, quality control samples; PCA, Principal Components Analysis; CID, collision-induced dissociation; EI, electronic impact; MSTFA, N-methyl-N-(trimethylsilyl)trifluoroacetamide; MTBE, Methyl tertiary-butyl ether; DCF, diclofenac; FLQ, flumequine; GC-MS, gas chromatography-mass spectrometry; UHPLC-QTOF, ultra-high performance liquid chromatography coupled to quadrupole time of flight; PCAs, polycyclic aromatic compounds; NSAID, nonsteroidal anti-inflammatory drug; CNS, central nervous system; AD, Alzheimer's disease; BBB, blood brain barrier; As, arsenic; HG, Mercury; Cd, Cadmium; Se, Selenium.

* Corresponding author.
E-mail address: tamara@dqcm.uhu.es (T. García-Barrera).
[1] Senior authors

https://doi.org/10.1016/j.jhazmat.2022.129443
Received 29 April 2022; Received in revised form 8 June 2022; Accepted 20 June 2022
Available online 25 June 2022

Metallomics
Gut microbiota

modulated several brain metabolic impairments caused by CC (*e.g.,* brain levels of the excitatory amino acid N-acetyl aspartic acid) by influencing mainly the metabolisms of purine, glycosylate and dicarboxylate, glutamate, glycerophospholipid, alanine and aspartate. Numerous associations were obtained between brain metabolites and gut microbes and they changed after Se-supplementation (*e.g., Lactobacillus* was positively associated with a brain ceramide, phosphoserine, phosphocholine, vitamin D3 derivative, fatty acids, malic acid, amino acids, and urea after the exposure, but not after Se-supplementation). Our results showed numerous evidences about the impact of CC on brain metabolome, the potential role of Se as an antagonist and their impact on the gut-brain axis. Further research is needed to understand the complex mechanism of action implied on CC-brain-microbiota interactions.

1. Introduction

Brain is an organ especially prone to be damaged by environmental pollutants in spite of the blood brain barrier (BBB), which prevents non-selective crossover of compounds in the circulating blood into the extracellular fluid of the central nervous system (CNS), where neurons dwell (Iqubal et al., 2020). Mercury (Hg) is one of the most widely known neurotoxic (Glaser et al., 2010), especially organic chemical species (Clarkson and Magos, 2006), but arsenic (As) can also induce neurotoxic effects such as encephalopathy, peripheral neuropathies, neurobehavioral alterations, and it has also been associated with neurodegeneration (Garza-Lombó et al., 2019; Grau-Perez et al., 2018). Also cadmium (Cd) has been linked to neurodegenerative diseases including Alzheimer's (AD) and Parkinson's diseases, multiple and amyotrophic lateral sclerosis (Branca et al., 2018). However, living beings are exposed to a multifaceted environment where pollutants can interact though antagonistic or synergistic mechanisms (García-Barrera et al., 2012; García-Sevillano et al., 2013a). Likewise, selenium (Se) is a recognized antagonist against Hg (García-Sevillano et al., 2015), As (Zwolak, 2020; García-Sevillano et al., 2013b) and Cd (Rodríguez-Moro et al., 2020), but also they can interact between each other (*e.g.*, Cd and As (García-Sevillano et al., 2014a) or As, Cd and Hg (García-Sevillano et al., 2014b)). Moreover, Se-supplementation has been shown to reduce the Aβ plaque deposition in the mouse brain (model APP/PS1) (Lovell et al., 2009) as well as the oxidative stress in the CNS, ameliorating the effects of AD (Iqbal et al., 2018). Recently, it has been pointed out that the nonsteroidal anti-inflammatory (NSAID) drug diclofenac (DCF) reduces the risk of AD (Stuve et al., 2020). Se-supplementation also has an impact on gut microbiota diversity, richness and composition (Arias-Borrego et al., 2019; Hrdina et al., 2009; Kim and Combs, 1997; Kasaikina et al., 2011; Zhai et al., 2018). Likewise, previous works with non-exposed Se-supplemented mice reported the connection of gut microbes with plasma selenoproteome and trace metal homeostasis (Callejón-Leblic et al., 2021), gut metabolites (Callejón-Leblic et al., 2022), testicular metabolome and selenoproteome (Ramírez-Acosta et al., 2022a) as well as brain metabolome and selenoproteome (Ramírez-Acosta et al., submitted for publication). Moreover, there is growing evidence about the crosstalk between gut microbiota through the so-called gut-brain axis (Burokas et al., 2015). However, the role of "chemical cocktails" on shaping brain metabolome and the possible connection with gut microbiota has not been precisely linked.

Herein, we studied the impact of a "chemical cocktail" including As, Cd, Hg and pharmaceuticals (PACs, flumequine and DCF) as well as Se-supplementation on mice brain metabolome and the associations with gut microbiota.

2. Experimental section

2.1. Animals, experimental design and dosage information

Animal handling was carried out at the Animal Experimentation Service of the University of Cordoba (SAEX-UCO), by qualified staff and following the European Community animal care guidelines. This work has received approval for research ethics from Ethical Committee of the University of Córdoba and Regional Government of Andalusia (Spain) and a proof/certificate of approval is available upon request (Code Num. 02–01–2019–001). The study design has already been described. Briefly, 8 weeks-male *Mus musculus* BALB/c mice were then randomly divided into three groups (n = 12): C, CC, and CC-Se and housed in pairs under controlled laboratory conditions for a total of 3 weeks, with free access to food and water as described previously (Callejón-Leblic et al., 2022). Mice in the control (C) group were fed a regular diet thorough the study. All mice, except the controls, received a mixture of flumequine-FLQ and DCF in the chow and Hg, Cd and As in the drinking water. The concentrations of DCF, FLQ, As, Cd and Hg were calculated for mice receiving daily doses of 20, 625, 3, 0.1, and 1 mg/kg, respectively, consistent with concentrations of environmental relevance (Fekadu et al., 2019; González-Gaya et al., 2022; Huygens et al., 2022). The chow of mice in the group CC-Se contained a Se supplement (sodium selenite, 0.65 mg/kg) (Zarrinpar et al., 2018; D'Amato et al., 2020). Fig. S1 summarizes the animal exposure experimental design.

2.2. Brain tissue preparation for metabolomic analysis

Sample preparation was carried out by a previously described method (Ramírez-Acosta et al., submitted for publication). Briefly, brain tissues were cryohomogenized into a ceramic mortar with liquid nitrogen. An amount of 30.0000 mg were weight, placed and homogenized into a 2 mL cryotube of a TissueLyser LT homogenizer (Qiagen, Germany) by adding a cold mixture (−20 ºC) of methanol/water (1:1, v/v). Metabolites were extracted from a 100 μL aliquot of the homogenate that was vortex mixed during 1 h with 400 μL of 80:20 (*v/v*) methanol/methyl *tert*-butyl ether (MTBE). Then, extracts were centrifuged at 4000 *g* for 20 min at 20ºC and the supernatants were separated. Two equal aliquots were separated for UHPLC-MS and GC-MS analysis and then, dried using SpeedVac concentrator system (Thermo Fisher Scientific, Bremen, Germany). Prior to GC-MS analysis, the dried extracts were submitted to derivatization in two steps, namely: (i) methoxymation, for the protection of carbonyl groups, by adding 50 μL of methoxyamine hydrochloride in pyridine at 20 mg mL^{-1} and incubating for 15 min at 80ºC. (ii) Silylation, by adding 50 μL of N-methyl-N-(trimethylsilyl)trifluoroacetamide (MSTFA) and incubating under the same conditions. For UHLC-MS analysis, the dried extracts were reconstituted in methanol:MTBE (80:20, *v/v*) and directly injected into the loop. To assess the stability of the analyses and reproducibility, quality control (QC) samples were prepared by pooling equal quantities of all brain extracts.

2.3. GC-MS metabolomic analysis

Gas chromatographic analysis was performed on a Trace GC ULTRA model gas chromatograph coupled to an ion trap mass spectrometer model ITQ900 (Thermo Fisher Scientific), using a Factor Four capillary column VF-5MS 30 m × 0.25 mm ID, with 0.25 μm of film thickness (Agilent technologies, Tokyo, Japan). The temperature of the column was initially set at 100 °C for 0.5 min and then ramped to 320 °C at 15 °C min^{-1} maintained for 2.8 min. Helium was used as a carrier gas supplied into the system at a constant flow rate of 1 mL min^{-1}. Injector

temperature was set to 200 ºC. Ionization of metabolites into the mass spectrometer was accomplished by electronic impact (EI) at 70 eV with a temperature filament of 230 ºC. To avoid the noisy signal of a big band from the solvent and other non-separated peaks, the filament was turned off for the first 4 min of the chromatogram. Finally, 1 μL of previously prepared metabolomic extract was injected in splitless mode and monitored in full scan mode in the *m/z* range 35–650.

2.4. UHPL-QTOF metabolomic analysis

A liquid chromatograh model Agilent 1290 Series equipped with a well-plate autosampler was used coupled to a QTOF model 6550 iFunnel system with a dual electrospray ion source handled in both positive and negative ionization modes (Agilent Technologies, Tokyo, Japan). In order to achieve a good separation of metabolites an inverse phase chromatography was performed with a mobile phase gradient of (A) water and (B) methanol/2-propanol (85:15, v/v). The analysis was carried out with a gradient from 82% to 100% of mobile phase B at a flow-rate of 0.4 mL min^{-1}. Thus, 5 μL of extracted brain samples were injected into an Agilent InfiniteLab Poroshell 120 EC-C18 chromatographic column (150 ×2.1 mm, 2.7 μm, Agilent Technologies) thermoregulated at 60ºC. The reference masses *m/z* 121.0509 and 922.0098, were constantly introduced into the system for mass correction in positive mode while the reference masses *m/z* 1033.9881 and 112.9856 were introduced for mass correction in negative ionization mode.

Full scan mode was recorded in the range of 100–1200 *m/z*. Other parameters were set as follows: capillary voltage (3.5 KV), drying gas flow rate (14 L min^{-1}), temperature (200 °C), gas nebulizer pressure (35 psi), sheath gas (350 ºC) and flow-rate (11 L min^{-1}). For positive and negative ionization modes, the fragmentor voltage was adjusted at 380 V. We used the Agilent Targeted MS/MS mode from MassHunter Data Acquisition software, to analyze a list containing the most significant metabolites. To this end, MS/MS scan rate was set at 1 spectrum s^{-1} with the same chromatographic conditions above described, using nitrogen as collision gas and voltages in the range of 10–40 V for the fragmentation of compounds. Data were acquired with a scan rate of 1.0 spectrum/second at centroid mode.

2.5. Annotation of brain metabolites

Data processing and statistical analysis was carried out as previously described (See supporting information, Table S1). For GC-MS metabolomic analysis, the version 8 NIST Mass Spectral Library was used to annotate metabolites, selecting only those with a probability > 80%. Target ions and at least two qualifiers (identifier ions) were selected from each mass spectrum. Those metabolites with a variation less than 20% in the area qualifier/target ion ratio per metabolite were selected. Kovat́s retention indexes (KRI) were calculated for the metabolites using a mixture of alkanes from C7-C40 (Sigma Aldrich, Germany). For UHLC-QTOF-MS metabolomic analysis, the software MassHunter version B.08.00 was used. To this end, the workflow "Compound Discovery" and the compound mining "Find by Molecular Features" were applied to the dataset. METLIN (http://metlin.scripps.edu) and HMDB (http://hmdb.*ca*) databases were used considering only those metabolites with a score higher than 90%. In addition, MS-MS experiments were performed with the same experimental conditions as applied for the primary analysis. Collision-induced dissociation (CID) fragmentation was used.

2.6. Gut microbiota profiling

Gut contents were sampled immediately after the killing of the mice and frozen in liquid N2. Aliquots of 80–100 mg were used for DNA isolation (Arias-Borrego et al., 2022). The gut microbiota profile obtained by 16 S rRNA amplicon sequencing previously described (Arias-Borrego et al., 2022) was used to combine with brain metabolomics in order to identify specific associations between brain metabolites and gut microbes shaped by the animal supplementation groups. Briefly, gut microbiota profiling was performed by the sequencing of the V3-V4 variable region of the 16 S rRNA gene following Illumina protocols. Amplicons were sequenced on a MiSeq-Illumina platform (FISABIO sequencing service, Valencia, Spain) using a 2 × 300 bp paired-end run (MiSeq Reagent kit v3). Negative control was included. Raw reads were processed and managed with the DADA2 pipeline and taxonomy was assigned with Silva v132 database. Tables with taxonomy at different levels (phylum, family and genus) were used for the integration with the available data in this study.

3. Results

3.1. Survival

Exposure to the contaminant cocktail resulted in a lethality of about 25% in animals consuming normal feed during treatment (CC *vs* C), which was reduced to 15% in mice that consumed a Se-supplemented diet. A Kaplan-Meier analysis (XLStat software, v. 2020.2.2.6533, Addinsoft) of the overall survival (OS) curves indicated that mice at the CC group had a significantly ($p = 0.016$) worse OS than their control counterparts. In contrast, the OS of mice in the CC+Se group did not differ from control ($p = 0.136$). The survival distribution functions and the results of the Kaplan-Meier analysis are shown in the Fig. S2.

3.2. Brain Mice Metabolome After Selenium Supplementation and Microbiota Depletion

Brain metabolomes were determined using the multiplatform based on UHPLC-QTOF-MS and GC-MS analysis, combining positive and negative ionization modes. The metabolomic analysis was evaluated using 6 quality control samples (QC). Principal Components Analysis (PCA) plots showed good stability and reliability of the results by clustering the QCs samples (Fig. S3). Principal Least Squares Discriminant Analysis (PLS-DA) showed good classifications between groups using the analytical metabolomics multiplatform (Fig. 1A, B and C). Moreover, pairwise comparisons were carried out to determine the metabolites that allowed discriminating groups. The 2D-PLS-DAs built from pairwise group comparison (Fig. S4) are shown in the Supporting Information.

A total of 49 brain metabolites (Table S2) were annotated combining GC-MS (13 metabolites) and $^{+/-}$ESI-MS (36 metabolites). KRIs were calculated for the identification of metabolites determined by GC-MS and they are summarized in Table S3. Fig. 1D collects the abundance of the metabolites annotated in C, CC and CC-Se groups in a heatmap diagram and Table S2 shows the complete list of metabolites with the *p*-values and fold changes (FC) among other information.

As can be seen in Fig. 1D and Table S2, there is a band of metabolites that decreased in mouse brain after the exposure to the CC (CC *vs* C FC<1). Among the **brain metabolites down-regulated by the CC exposure, several ones increased the levels after Se-supplementation** to levels close to the C group or even not significantly different (FC CC-Se *vs* CC greater than those for CC *vs* C comparison). This last group of metabolites included (compound class and FC CC-Se *vs* CC in brackets): monopalmitin (*monoglyceride,* 2.18-fold), cer(d16:1/24:0) (*ceramide, N-acylsphingosine,* 2.70-fold), deoxyrubroskyrin (*anthracene, anthraquinone,* 1.94-fold) and undecyl isobutyrate (*fatty acyl, fatty ester*, 3.90-fold). There are other **brain metabolites up-regulated by the CC exposure that was down-regulated by Se-supplementation** (FC CC-Se *vs* CC lower than those for CC *vs* C comparison) including (compound class and FC CC-Se *vs* CC in brackets): N-acetyl aspartic acid (*excitatory amino acid,* 0.51-fold) and phosphoric acid (*acid anhydride, acrylic acid anhydride,* 1.47-fold). There were other **brain metabolites altered by Se-supplementation, but that were not significantly impaired after the CC exposure when this last group is compared with the C group** (compound class and FC CC-Se *vs* C in brackets): spisulosine (*sphingolipids, organonitrogen compound, amine,* 2.15-fold),

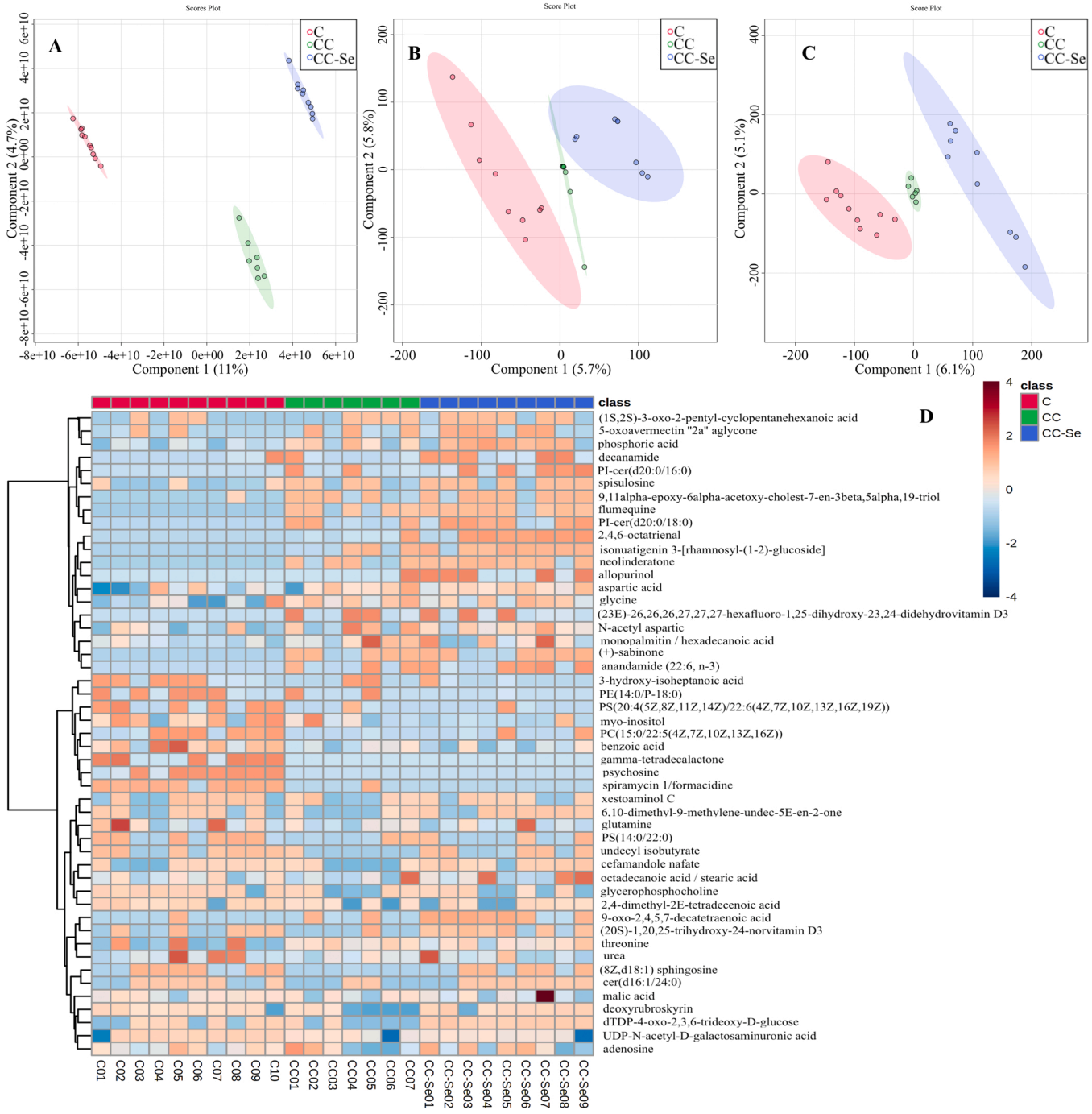

Fig. 1. A) 3D-PLS-DA of brain samples corresponding to GC-MS analysis, B) UHPLC-ESI$^+$-QTOF-MS and C) UHPLC-ESI$^-$-QTOF-MS. C: red dots, CC: green dots, CC-Se: blue dots. D) Cluster heatmap of brain metabolites from C, CC and CC-Se mice. Metabolites are represented in rows and mice of different groups in columns. Red and blue colors show increased and decreased levels of brain metabolites, respectively.

xestoaminol C (*organonitrogen compound, amine*, 1.06-fold), 5-oxoavermectin "2a" aglycone (*macrolide and analogues, milbemycins*, 2.88-fold), decanamide (*fatty acyl, fatty amide,* 4.77-fold), (3-oxo2-pentyl-cyclopentanehexanoic acid (*fatty acyl, octadecanoid,* 2.36-fold), 9-oxo-2,4,5,7-decatetranoic acid (*medium chain fatty acid*, 8.47-fold), PS(14:0/22:0) (*glycerophospholipid, glycerophosphcholine, phosphatidylserine,* 0.51-fold), PE(14:0/P-18:0) (*glycerophospholipid, glycerophosphoethanolamine,* 0.02-fold), PS(20:4/22:6) (*glycerophospholipid, glycerophosphcholine, phosphatidylserine*, 0.19-fold) and malic acid (*hydroxyl acid derivative*, 0.63-fold). There were other **brain metabolites impaired by the CC that Se-supplementation cannot antagonize or even it has a synergistic action** (compound class and FC CC *vs* C in brackets): glycerophosphocholine (*glycerophospholipid, glycerophosphocholine*, 0.65-fold), 9,11alpha-epoxy-6alpha-acetoxy-cholest-7-en-3beta,5alpha,19-triol (*sterol, cholesterol derivative*, 7.96-fold), (8Z,d18:1)sphingosine (*sphingolipid, sphingoid base,* 0.02-fold), spiramycin 1 (*organooxygen compound, carbohydrate derivative*, 0.16-fold), PC(15:0/22:5) (*phosphocholine, glycerophosphocholine*, 0.02-fold), UDP-N-acetyl-D-galactosaminuronic acid (*pyrimidine nucleotide sugar*, 0.94-fold), 3-hydroxy-isoheptanoic acid (*fatty acids and conjugates,* 0.65-fold), adenosine (*purine nucleoside,* 0.18-fold), aspartic acid (*amino acid*, 16.18-fold), benzoic acid (*benzene derivatives*, 71.44-fold), glutamine (*carboxylic acid*

derivative, amino acid, 0.74-fold), glycine (*carboxylic acid derivative, amino acid*¸ 0.91-fold), myo-inositol (*organooxygen compound, alcohols and polyols,* 0.30-fold), N-acetyl-aspartic acid (*excitatory amino acid,* 3.21-fold), stearic acid (*fatty acyls, fatty acids and conjugates,* 0.06-fold), threonine (*carboxylic acid and derivatives, amino acid,* 43.73-fold) and urea (*organic carbonic acids and derivatives*, ureas, 14.48-fold).

Finally, the FC of several metabolites cannot be calculated because they were **absent in the control grou**p. This is the case of flumequine, a pharmaceutical included in the chemical cocktail, which was not present in mice of the C group, and for this reason there are not FC for CC *vs* C or CC-Se *vs* C (Table S2). **Metabolites absent in the control group** are (compound class and FC CC-Se *vs* C in brackets, when significant differences were found): flumequine (*quinolones and derivatives,* 1.27-fold), PI-cer(d20:0/16:0) (*phosphosphingolipid, ceramide phosphoinositol,* 1.96-fold), PI-cer(d20:0/18:0) (1.62-fold), neolinderatone (*poliketides, flavanones* 1.55-fold), sabinone (*prenol lipids, monoterpenoids*), 2,4,6-octatrienal (*fatty acids, aldehyde*), 26,26,26,27,27,27-hexafluoro-1,25-dihydroxy-23,24-didehydrovitamin D3 (*vitamin D derivatives*), allopurinol (*pyrazolopyridimines,* 4-fold), isonuatigenin 3-[rhamnosyl-(1−2)-glucoside] (*steroids, steroidal glycosides*) and anandamide (22:6,n-3) (*ethanolamines, N-acylethanolamine*).

Moreover, the most impaired metabolic routes in the group CC and the changes after Se-supplementation were evaluated using the MetaboAnalyst 5.0 (metaboanalyst.*ca*) tool. The pathway analysis showed a total of 6 significantly altered routes in mouse brain metabolome after the exposure to CC (Fig. 2 A) including arginine and aminoacyl-tRNA biosynthesis, and the metabolisms of glycine, serine and threonine, alanine, aspartate and glutamate, glyoxylate and dicarboxylate and purine. Otherwise, the most significantly altered pathways after the exposure of the CC in Se-supplemented mice (Fig. 2B) are arginine and aminoacyl-tRNA biosynthesis and the metabolism of glycine, serine and threonine. Table S4 collects *p*-values, the numbers of hits and the impact of the affected metabolic routes by the impaired metabolites found CC and CC-Se groups.

3.3. Brain metabolome is associated with gut microbiota and affected by the "chemical cocktail" and selenium supplementation

In previous works, we described changes in the gut microbiota composition and diversity in mice as a result of Se-supplementation in conventional and microbiota depleted mice models (Callejón-Leblic et al., 2021), as well as after the CC exposure and/or Se-supplementation (Arias-Borrego et al., 2022). Moreover, we found that Se-supplementation increased the relative abundance of a number of health-relevant taxa, especially in the microbiota depleted mice model (Callejón-Leblic et al., 2021). A total of 66 different genera and their relative abundance (Table S5) were determined in C, CC, CC-Se mice groups. In this work, specific associations (Table S6, Fig. 2 C and D) between the relative abundance of the identified bacterial genera and brain metabolites in the different experimental groups were analyzed. Our results suggest that brain metabolome are related with gut microbiota composition and that those associations are perturbed by the exposure to the CC and changed by Se-supplementation.

We found distinct microbial shift according to the supplementation groups: (i) the first one, extensively increased the associations with brain metabolites after the exposure to the CC, but they decreased and changed them after Se-supplementation (*e.g., Lachnospiraceae NK4A136 group, Lactobacillus, Mucispirillum,* several members of the families

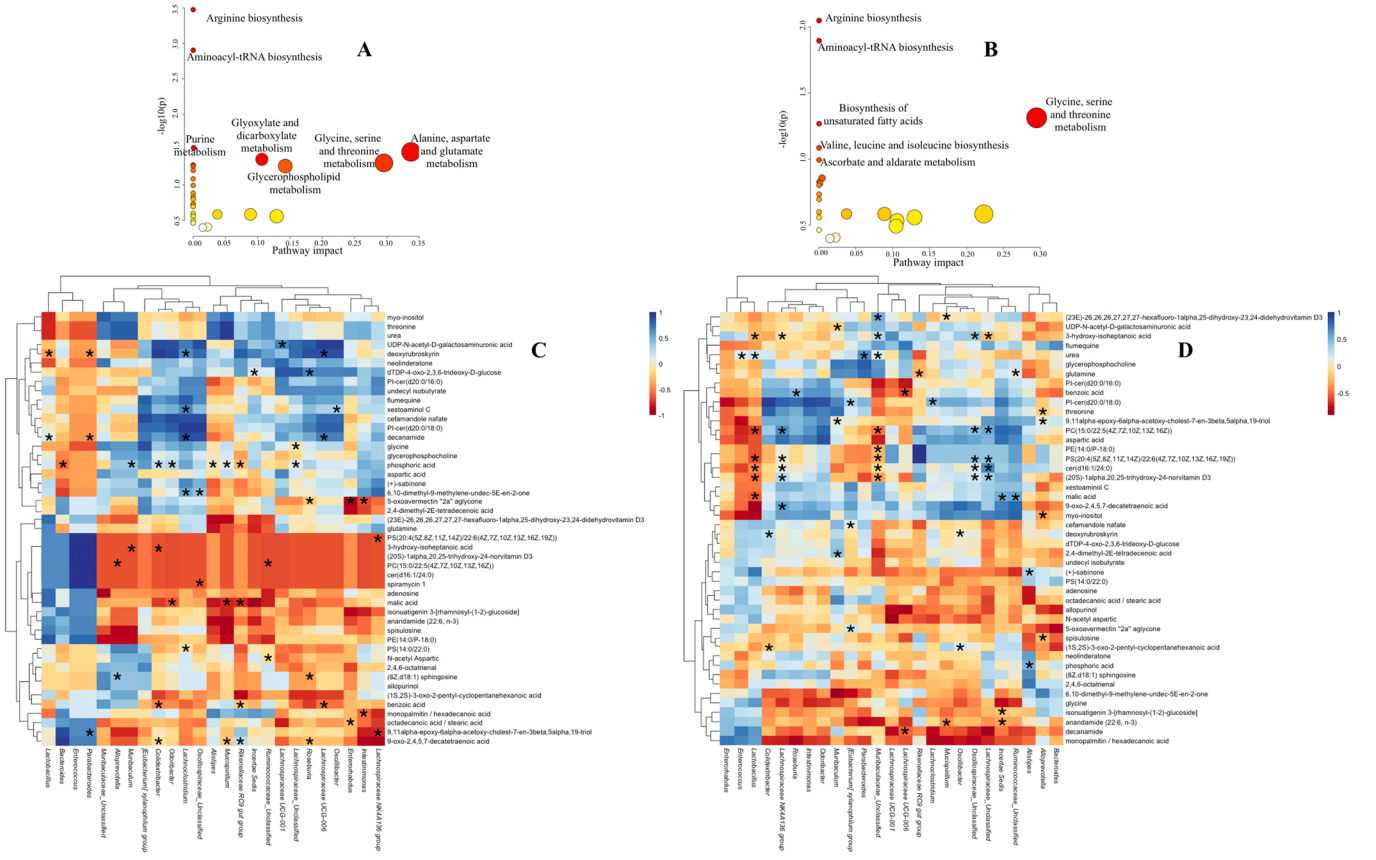

Fig. 2. A) Pathway analysis plots showing the most impaired metabolic routes in CC and B) CC-Se groups. The *p*-values calculated from the enrichment analysis are indicated by a color gradient: from white (highest *p*-value) to red (lowest *p*-value), while the pathway impact value calculated from pathway topology analysis is indicated by dot size. C) Spearman correlation heatmaps showing the associations between brain metabolites and gut microbiota in CC and D) CC-Se groups. Blue and red colors indicate positive and negative correlations, respectively.

Oscillospiraceae, *Peptococcaceae*, *Muribaculaceae, Tannerellaceae*); (ii) the second group includes genera that decreased the associations with brain metabolome after CC exposure, but they increased after Se-supplementation (*e.g., Roseburia*) and (iii) genera without any association with brain metabolome after CC exposure, but that they widely increased after Se-supplementation (*e.g., Escherichia-Shigella*, *Lachnospiraceae UCG-001*, *Intestinimonas, Enterorhabdus, Acetatifactor*).

Therefore, we found specific associations between *Lachnospiraceae NK4A136 group* and only two brain metabolites in the C group (Table S6), while in the CC group they increased up to 7 negative correlations with brain metabolites including PS(20:4/22:6) (phosphatidylserine), cer(d16:1/24:0) (ceramide), PC(15:0/22:5) (phosphatidylcholine), 9-oxo-2,4,5,7-decatetraenoic acid and 3-hydroxy-isoheptanoic acid (fatty acids and conjugates) and (20 S)−1,20,25-trihydroxy-24-norvitamin D3 (fat-soluble vitamin). After Se-supplementation of CC mice, this genus was associated with myo-inositol (organooxygen compound), aspartic acid (neurotransmitter) and monopalmitin (monoglyceride). *Lactobacillus* genus also increased the associations with brain metabolites in CC group being the most significant correlations (mainly positives) with almost the same brain metabolites that *Lachnospiraceae NK4A136 group*, such as PS(20:4/22:6), cer(d16:1/24:0), PC(15:0/22:5), 1,20,25-trihydroxy-24-norvitamin D3 and other new metabolites including 3-hydroxy-isoheptanoic acid (fatty acids and derivatives), malic acid (dicarboxylic acid), proline (amino acid) and urea (organic carbonic acids and derivatives). After Se-supplementation, this genus was positively associated with monopalmitin and negatively with PI-cer(d20:0/18:0) (phosphatidylinositol ceramide) and 9-oxo-2,4,5,7-decatetraenoic acid (fatty acids and conjugates). *Mucispirillum* genus was also negative associated after CC exposure, with brain 26,26,26,27,27,27-hexafluoro-1,25-dihydroxy-23,24-didehydrovitamin D3 (vitamin D3 derivative) as well as with anandamide (22:6, n-3) (endocanabinoid) and threonine (amino acid), while after Se-supplementation this genus was only associated with monopalmitin.

The associations of *Roseburia* with brain metabolites decreased to only one negative correlation with benzoic acid in brain after CC exposure and to three associations after Se-supplementation with 9-oxo-2,4,5,7-decatetraenoic acid, monopalmitin and myo-inositol.

The genera *Escherichia-Shigella*, *Lachnospiraceae UCG-001* and *Intestinimonas* genera did not present any association with brain metabolome after CC exposure, but they were associated with brain metabolites after Se-supplementation. Thus, the first genus was associated, after Se-supplementation with phosphoric acid and 3-hydroxy-isoheptanoic acid, while the second one with four metabolites including PE(14:0 P-18:0), PS(20:4/22:6), N-acetyl aspartic acid and cefamandole nafate, and the last with aspartic acid and benzoic acid.

4. Discussion

Although the impact of metals (Xu et al., 2015; Wang et al., 2021), selenium (Ramírez-Acosta et al., submitted for publication; Rodríguez-Moro et al., 2019) and organic xenobiotics (Rodríguez-Moro et al., 2019) in brain metabolome has been previously reported, limited evidence is available about the join effect of pollutants in brain metabolome as well as the possible influence of Se-supplementation and the crosstalk with gut microbiota.

4.1. Brain metabolome is shaped by the exposure to the "chemical cocktail" and selenium supplementation

Our results demonstrated that the exposure to the CC strongly affects the brain metabolome by the up- or down-regulation of metabolites that belongs to compound classes very related with brain function, such as excitatory amino acids, ceramides, fatty acyls and monoglycerides, among others and that Se-supplementation modulated the impairments. Likewise, N-acetyl aspartic acid was up-regulated by the CC exposure, but Se-supplementation modulated the levels to that in the control group, since there were not significant differences between these two groups. The excitatory amino acid N-acetyl aspartic acid, accounts for around one thousandth of the wet weight of human brain and appears to be restricted solely to neurons being involved in important functions such as myelin production, regulation of neuronal protein synthesis or the metabolism of several neurotransmitters such as aspartate or N-acetyl-aspartyl-glutamate (Birken and Oldendorf, 1989). Phosphoric acid was also up-regulated by the exposure and modulated by Se-supplementation, but interestingly, this metabolite was up-regulated after Se-supplementation in non-exposed mice (Ramírez-Acosta et al., submitted for publication).

Se-supplementation also modulated the down-regulation of the brain ceramide cer(d16:1/24:0). Ceramides are precursors of all complex sphingolipids, which intracellular levels must be fine-tuned since changes in the sphingolipid-ceramide profile play a role in the development of neurological, age-related, and neuroinflammatory disorders (Mencarelli and Martinez-Martinez, 2013). Other metabolites down-regulated by CC and modulated by Se-supplementation belongs to the compound classes of monoglycerides and fatty acyls, that are also important for brain (Ramírez-Acosta et al., submitted for publication). There were other group of metabolites modulated by Se-supplementation in exposed mice that were not affected by the CC in mice fed rodent diet. Likewise, Se-supplementation up-regulated in brain the sphingolipids spirulosine, which inhibits the proliferation of numerous cancer cell lines (Pruett et al., 2008) and xestoaminol C, which affect the resistance of rat renal and mesenteric vessels through G protein-coupled receptor (Bischoff et al., 2000). Se also increased the brain levels of a neurotransmitter and other metabolites classified as fatty acyls and medium chain fatty acids, and down-regulated malic acid and several glycerophospholipids including PS and PE, whose composition is very important for the neural membranes functionality, fluidity and permeability, and that the alterations in neural membrane glycerophospholipid composition have been reported to occur in neurological disorders (Farooqui et al., 2000). Other brain metabolites were down-regulated by the exposure to the CC and Se-supplementation did not modulate the levels, including glycerophosphocholine and a PC, that usually are elevated in brain during neurodegeneration due to the breakdown of membrane phospholipids (Walter et al., 2004). Interestingly, the CC exposure strongly decreased the brain levels of PC (15:0/22:5) (0.02-fold), that was previously associated with disturbed condition in brain cells (li Yin et al., 2019; Chai et al., 2021) and (8Z, d18:1)sphingosine (0.02-fold). Otherwise, the CC exposure strongly up-regulated the levels of aspartic acid (16.18-fold), considered one of the main excitatory amino acids in CNS (Wang et al., 2021) that was found upregulated in adverse conditions (Ji et al., 2017; Dai et al., 2016), benzoic acid (71.44-fold), known to be up-regulated after As exposure (Sun et al., 2021) and mainly excreted by kidneys, threonine (43.73-fold), previously reported to be elevated as response to neurotoxicity as well as in an Alzheimer's disease model (Fu et al., 2017; Hu et al., 2012), and urea (14.48-fold), previously described to be increased in serum after Abx treatment (Xu et al., 2021).

The pathway analysis plots clearly show that Se-supplementation ameliorated several metabolic pathways impaired by the CC exposure. Likewise, Se-supplementation ameliorated the impact of the CC on the purine metabolism, glycosylate and dicarboxylate metabolism, glycerophospholipid metabolism, alanine, aspartate and glutamate metabolism. Otherwise, Se-supplementation acts mainly on biosynthesis of unsaturated fatty acids, glycine, serine and threonine metabolism, valine, leucine and isoleucine biosynthesis and ascorbate and aldarate metabolism.

4.2. Specific gut microbes associated with multiple brain metabolites

In this work, numerous associations between brain metabolites and gut microbiota were found at genus level. As commented before, there

are genera that widely increased or decreased the number of associations with brain metabolites after the exposure to the CC and that Se-supplementation restored this behavior. Among these genera, *Lachnospiraceae NK4A136 group* has been previously claimed as a potential butyrate producer and thus, a promising therapeutic target in dementia because it is lower in these patients compared to controls (Stadlbauer et al., 2020). In our previous work (Callejón-Leblic et al., 2021), we demonstrated that *Lachnospiraceae* family increased after Se-supplementation. In the present work, this genus is negatively associated in CC group with important brain metabolites including PS, PC, ceramides, fatty acids and conjugates and fat-soluble vitamins. After Se-supplementation these associations disappears and this genus positively correlated with a fat-soluble vitamin, myo-inositol and the neurotransmitter aspartic acid, and negatively with monopalmitin. Another genus extensively associated with brain metabolites is *Lactobacillus genus,* a potentially health-relevant taxa, which also increased after Se-Supplementation according to our previous results (Callejón-Leblic et al., 2021). After the CC exposure, this genus was positively associated with a brain ceramide, PS, PC, vitamin D3 derivative, fatty acids, malic acid, amino acids, and urea. After Se-supplementation, these correlations disappeared and it was negatively correlated with a PI and a fatty acid, and positively with monopalmitin. *Mucispirillum* genus was also negative associated after CC exposure, with brain vitamin D3 derivative, an endocanabinoid and an amino acid, while after Se-supplementation this genus only correlated with brain monopalmitin. Previously, this genus has been linked to sperm activity and testosterone, as well as glutathione peroxidase and selenoalbumin in testicular tissue (Ramírez-Acosta et al., 2022a). The associations of *Roseburia* genus with brain metabolites decreased after the CC to be only correlated with brain benzoic acid, but Se-supplementation increased the association to brain metabolome including 9-oxo-2,4,5,7-decatetraenoic acid, monopalmitin and myo-inositol. This genus has been previously related with depressive symptoms in patients with the body mass index (BMI) in patients with anorexia nervosa (AN) (Di Lodovico et al., 2021) and with major depressive disorder (Ye et al., 2021). The genus *Escherichia-Shigella* genus did not correlated with any brain metabolites after CC exposure, but after Se-supplementation, they were positively associated with phosphoric acid and 3-hydroxy-isoheptanoic acid. This genus has been associated with reproductive endocrine systemś sex hormones, as well as testicular selenoprotein P (Ramírez-Acosta et al., 2022a). In the present work, Se-supplementation induced the association with a brain PE, a PS, N-acetyl aspartic among others.

4.3. Specific brain metabolites associated with multiple gut microbes

Interestingly, there were brain metabolites altered after the CC and/or Se-supplementation that were associated repeatedly with a great number of gut microbes. These metabolites have been previously related with important brain functions and neurotoxicity. Among the class of *glycerophospholipids*, the phosphatidylserine PS(20:4/22:6) in mice brain, was associated with several genera after the exposure to the CC and with some others after Se-supplementation. In addition, the PS (14:00/22:0) was also associated with several genera in the control and CC-Se groups. There were no other PSs associated with gut bacteria in this study. PS(20:4/22:6) consists of one chain of arachidonic acid and one chain of docosahexaenoic acid and the greatest concentration is located in myelin from brain tissue (FooDB, 2011). In general, PSs are required for healthy nerve cell membranes and myelin (Glade and Smith, 2015). The *glycerophospholipid* glycerophosphocholine (GPCh), was associated with several genera in the C and CC-Se groups. Furthermore, the phosphatidylcholine PC(15:0/22:5) in mice brain was also associated with a great number of genera, but only in the CC and C groups. It is well-known that during neurodegeneration membrane phospholipids are breakdown and choline metabolites increases. These are the water-soluble metabolites of PC and includes GPCh, phosphocholine (PCh), and choline (Ch) (Walter et al., 2004). Only two *ceramides* in mice brain were associated with gut microbiota, the cer (16:1/24:0) and cer(20:0/18:0) in the CC and Se-CC groups, as well as their corresponding phosphatidylinositol ceramides (PI-cer(20:0/18:0) and PI-cer(16.1:24:0), which belongs to the class of *phosphosphingolipids*. The *sphingolipid* psychosine in brain was associated with several genera only in the control group. Ceramides are sphingolipids precursors as well as powerful signaling molecules that mediate crucial processes in cellular pathophysiology (Mencarelli and Martinez-Martinez, 2013). Alteration of the sphingolipid-ceramide profile led to the development of neurological, age-related and neuroinflammatory diseases (Mencarelli and Martinez-Martinez, 2013). The vitamin D3 derivatives 26,26,26,27,27,27-hexafluoro-1,25-dihydroxy-23,24-didehydrovitamin D3 and 1,20,25-trihydroxy-24-norvitamin D3 were mainly negatively associated with several genera in the CC and CC-Se groups. The effect of 26,26,26,27,27,27-Hexafluoro-1,25-dihydroxyvitamin D3 on the expression of vitamin-D-responsive genes in vitamin-D-deficient mice has been previously reported (Yoshimura et al., 1998). In fact, Vitamin D has neuroprotective properties, modulates the immune system, and aids calcium homeostasis. It also has a role in the regulation of a wide number of genes that are crucial for brain function. Although vitamin D is classified as a vitamin, it acts as well as a neurosteroid and has key role in the brain (Anjum et al., 2018). Also, the neurotransmitter aspartic acid in brain was associated with several members of gut microbiota in the CC-Se mice. Other brain metabolites widely associated with gut microbes were malic acid (*hydroxy acid and derivatives*), monopalmitin (*monoradylglycerols*), myo-inositol (*alcohol*), 3-hydroxy-isoheptanoic acid and stearic acids (*fatty acyls*), the amino acids glycine, aspartic acid, threonine, proline and glutamine (*aminoacids*), UDP-N-acetyl-D-galactosaminuronic acid (*nucleotide-sugar*), benzoic acid, adenosine (*purine nucleoside*), spisulosine (*sphingolipids, organonitrogen compounds*), urea and phosphoric acid. Finally, the brain metabolite that presented more associations with gut microbiota was the fatty acid 9-oxo-2,4,5,7-decatetraenoic acid.

5. Conclusions

Untargeted brain metabolomics combining GC-MS and UHPLC-QTOF-MS revealed important impairments caused by CC that were modulated by Se supplementation. These metabolites belong to key compound classes for brain function such as excitatory amino acids, ceramides, fatty acyls and monoglycerides, among others. Interestingly, novel associations were determined between brain metabolites and gut microbes suggesting an intertwined mechanism, but they also disappeared or changed after Se supplementation. Our results demonstrated that there is a potential key interaction between Se intake–microbiota–brain metabolites with effects on the host health at multiple levels including gut-brain axis and reproductive health. However, the precise link needs to be ascertained and further studies targeted to the specific mechanisms are needed.

Funding Sources

This work was supported by the projects: PG2018–096608-B-C21 and PID2021-123073NB-C21 from the Spanish Ministry of Science and Innovation (MICIN). Generación del Conocimiento. MCI/AEI/ FEDER "Una manera de hacer Europa", UHU-1256905 and UHU-202009 from the FEDER Andalusian Operative Program 2014–2020 (Ministry of Economy, Knowledge, Business and Universities, Regional Government of Andalusia, Spain). The authors are grateful to FEDER (European Community) for financial support, Grant UNHU13–1E-1611. CPM thanks MICIN for a predoctoral grant (ref. PRE2019–091650). Funding for open access charge: Universidad de Huelva / CBUA. The authors would like to acknowledge the support from The Ramón Areces Foundation (ref. CIVP19A5918).

CRediT authorship contribution statement

C. Parra-Martínez: Formal analysis, Data curation, Visualization, Validation, Investigation, Writing – review & editing. **M. Selma-Royo:** Formal analysis, Data curation, Visualization, Investigation, Methodology, Writing – review & editing. **B. Callejón-Leblic:** Visualization, Formal analysis, Data curation, Methodology, Supervision, Writing – review & editing. **M.C. Collado:** Conceptualization, Methodology, Writing – original draft, Writing – review & editing. **N. Abril:** Conceptualization, Formal analysis, Investigation, Methodology, Writing – original draft, Writing – review & editing. **T. García-Barrera:** Conceptualization, Supervision, Methodology, Writing – original draft, Writing – review & editing, Funding acquisition, Project administration.

Author Contributions

The manuscript was written through contributions of all authors. All authors have given approval to the final version of the manuscript.

Declaration of Competing Interest

The authors declare that they have no known competing financial interests or personal relationships that could have appeared to influence the work reported in this paper.

Data Availability

Data will be made available on request.

Appendix A. Supporting information

Supplementary data associated with this article can be found in the online version at doi:10.1016/j.jhazmat.2022.129443.

References

Anjum, I., Jaffery, S.S., Fayyaz, M., Samoo, Z., Anjum, S., 2018. The role of vitamin D in brain health: a mini literature review. Cureus 10. https://doi.org/10.7759/CUREUS.2960.

Arias-Borrego, A., Callejón-Leblic, B., Calatayud, M., Gómez-Ariza, J.L., Collado, M.C., García-Barrera, T., 2019. Insights into cancer and neurodegenerative diseases through selenoproteins and the connection with gut microbiota - current analytical methodologies. Expert Rev. Proteom. 16, 805–814. https://doi.org/10.1080/14789450.2019.1664292.

Arias-Borrego, A., Selma-Royo, M., Collado, M.C., Abril, N., García-Barrera, T., 2022. Impact of "chemical cocktails" exposure in shaping mice gut microbiota and the role selenium supplementation combining metallomics, metabolomics and metataxonomics. J. Hazard. Mater.

Birken, D.L., Oldendorf, W.H., 1989. N-Acetyl-L-Aspartic acid: a literature review of a compound prominent in 1H NMR spectroscopic studies of brain. Neurosci. Biobehav. Rev. 13, 23–31. https://doi.org/10.1016/S0149-7634(89)80048-X.

Bischoff, A., Czyborra, P., Meyer Zu Heringdorf, D., Jakobs, K.H., Michel, M.C., 2000. Sphingosine-1-phosphate reduces rat renal and mesenteric blood flow in vivo in a pertussis toxin-sensitive manner. Br. J. Pharm. 130, 1878–1883. https://doi.org/10.1038/SJ.BJP.0703516.

Branca, J.J.V., Morucci, G., Pacini, A., 2018. Cadmium-induced neurotoxicity: still much ado. Neural Regen. Res. 13, 1879–1882. https://doi.org/10.4103/1673-5374.239434.

Burokas, A., Moloney, R.D., Dinan, T.G., Cryan, J.F., 2015. Microbiota regulation of the Mammalian gut-brain axis. Adv. Appl. Microbiol 91, 1–62. https://doi.org/10.1016/BS.AAMBS.2015.02.001.

Callejón-Leblic, B., Selma-Royo, M., Collado, M.C., Abril, N., García-Barrera, T., 2021. Impact of antibiotic-induced depletion of gut microbiota and selenium supplementation on plasma selenoproteome and metal homeostasis in a mice model. J. Agric. Food Chem. 69, 7652–7662. https://doi.org/10.1021/ACS.JAFC.1C02622.

Callejón-Leblic, B., Selma-Royo, M., Collado, M.C., Gómez-Ariza, J.L., Abril, N., García-Barrera, T., 2022. Untargeted gut metabolomics to delve the interplay between selenium supplementation and gut microbiota. J. Proteome Res. 21 https://doi.org/10.1021/ACS.JPROTEOME.1C00411.

Chai, C., Jin, B., Yan, Y., Yuan, Q., Wen, H., Tao, W., Cui, X., Shan, C., Yu, S., 2021. Antidepressant effect of Zhi-zi-chi decoction on CUMS mice and elucidation of its signaling pathway. J. Ethnopharmacol. 266, 113283 https://doi.org/10.1016/J.JEP.2020.113283.

Clarkson, T.W., Magos, L., 2006. The toxicology of mercury and its chemical compounds. Crit. Rev. Toxicol. 36, 609–662. https://doi.org/10.1080/10408440600845619.

D'Amato, A., Di Cesare Mannelli, L., Lucarini, E., Man, A.L., Le Gall, G., Branca, J.J.V., Ghelardini, C., Amedei, A., Bertelli, E., Regoli, M., Pacini, A., Luciani, G., Gallina, P., Altera, A., Narbad, A., Gulisano, M., Hoyles, L., Vauzour, D., Nicoletti, C., 2020. Faecal microbiota transplant from aged donor mice affects spatial learning and memory via modulating hippocampal synaptic plasticity- and neurotransmission-related proteins in young recipients. Microbiome 8. https://doi.org/10.1186/S40168-020-00914-W.

Dai, H., Xia, Y.Y., Ting-Li Han, T.L.H., Philip, P.N.B., Baker, N., Tang, X., Zhang, R.Y., Du, H., Cai, T.J., Cheng, S.Q., 2016. Effect of chronic arsenic exposure on mouse brain tissue and serum metabolomics. Nan Fang. Yi Ke Da Xue Xue Bao. 36, 1192–1197. https://europepmc.org/article/med/27687649 (Accessed 8 April 2022).

Di Lodovico, L., Mondot, S., Doré, J., Mack, I., Hanachi, M., Gorwood, P., 2021. Anorexia nervosa and gut microbiota: a systematic review and quantitative synthesis of pooled microbiological data. Prog. Neuropsychopharmacol. Biol. Psychiatry 106. https://doi.org/10.1016/J.PNPBP.2020.110114.

Farooqui, A.A., Horrocks, L.A., Farooqui, T., 2000. Glycerophospholipids in brain: their metabolism, incorporation into membranes, functions, and involvement in neurological disorders. Chem. Phys. Lipids 106, 1–29. https://doi.org/10.1016/S0009-3084(00)00128-6.

Fekadu, S., Alemayehu, E., Dewil, R., Van der Bruggen, B., 2019. Pharmaceuticals in freshwater aquatic environments: a comparison of the African and European challenge. Sci. Total Environ. 654, 324–337. https://doi.org/10.1016/J.SCITOTENV.2018.11.072.

FooDB, Showing Compound PS(20:4(5Z,8Z,11Z,14Z)/22:6(4Z,7Z,10Z,13Z,16Z,19Z)) (FDB029055), (2011). https://foodb.ca/compounds/FDB029055 (Accessed 28 April 2022).

Fu, Y., Si, Z., Li, P., Li, M., Zhao, H., Jiang, L., Xing, Y., Hong, W., Ruan, L., Wang, J.S., 2017. Acute psychoactive and toxic effects of D. metel on mice explained by 1H NMR based metabolomics approach, 2017 324 Metab. Brain Dis. 32, 1295–1309. https://doi.org/10.1007/S11011-017-0038-9.

García-Barrera, T., Gómez-Ariza, J.L., González-Fernández, M., Moreno, F., García-Sevillano, M.A., Gómez-Jacinto, V., 2012. Biological responses related to agonistic, antagonistic and synergistic interactions of chemical species. Anal. Bioanal. Chem. 403, 2237–2253. https://doi.org/10.1007/S00216-012-5776-2.

García-Sevillano, M.A., Jara-Biedma, R., González-Fernández, M., García-Barrera, T., Gómez-Ariza, J.L., 2013a. Metal interactions in mice under environmental stress. Biometals 26, 651–666. https://doi.org/10.1007/S10534-013-9642-2.

García-Sevillano, M.A., García-Barrera, T., Navarro, F., Gómez-Ariza, J.L., 2013b. Analysis of the biological response of mouse liver (Mus musculus) exposed to As2O3 based on integrated -omics approaches. Metallomics 5, 1644–1655. https://doi.org/10.1039/C3MT00186E.

García-Sevillano, M.A., García-Barrera, T., Gómez-Ariza, J.L., 2014b. Application of metallomic and metabolomic approaches in exposure experiments on laboratory mice for environmental metal toxicity assessment. Metallomics 6, 237–248. https://doi.org/10.1039/C3MT00302G.

García-Sevillano, M.A., Rodríguez-Moro, G., García-Barrera, T., Navarro, F., Gómez-Ariza, J.L., 2015. Biological interactions between mercury and selenium in distribution and detoxification processes in mice under controlled exposure. Effects on selenoprotein. Chem. Biol. Interact. 229, 82–90. https://doi.org/10.1016/J.CBI.2015.02.001.

García-Sevillano, M.Á., García-Barrera, T., Navarro-Roldán, F., Montero-Lobato, Z., Gómez-Ariza, J.L., 2014a. A combination of metallomics and metabolomics studies to evaluate the effects of metal interactions in mammals. Application to Mus musculus mice under arsenic/cadmium exposure. J. Proteom. 104, 66–79. https://doi.org/10.1016/J.JPROT.2014.02.011.

Garza-Lombó, C., Pappa, A., Panayiotidis, M.I., Gonsebatt, M.E., Franco, R., 2019. Arsenic-induced neurotoxicity: a mechanistic appraisal. J. Biol. Inorg. Chem. 24, 1305–1316. https://doi.org/10.1007/S00775-019-01740-8.

Glade, M.J., Smith, K., 2015. Phosphatidylserine and the human brain. Nutrition 31, 781–786. https://doi.org/10.1016/J.NUT.2014.10.014.

Glaser, V., Leipnitz, G., Straliotto, M.R., Oliveira, J., dos Santos, V.V., Wannmacher, C.M. D., de Bem, A.F., Rocha, J.B.T., Farina, M., Latini, A., 2010. Oxidative stress-mediated inhibition of brain creatine kinase activity by methylmercury. Neurotoxicology 31, 454–460. https://doi.org/10.1016/J.NEURO.2010.05.012.

González-Gaya, B., García-Bueno, N., Buelow, E., Marin, A., Rico, A., 2022. Effects of aquaculture waste feeds and antibiotics on marine benthic ecosystems in the Mediterranean Sea. Sci. Total Environ. 806 https://doi.org/10.1016/J.SCITOTENV.2021.151190.

Grau-Perez, M., Navas-Acien, A., Galan-Chilet, I., Briongos-Figuero, L.S., Morchon-Simon, D., Bermudez, J.D., Crainiceanu, C.M., de Marco, G., Rentero-Garrido, P., Garcia-Barrera, T., Gomez-Ariza, J.L., Casasnovas, J.A., Martin-Escudero, J.C., Redon, J., Chaves, F.J., Tellez-Plaza, M., 2018. Arsenic exposure, diabetes-related genes and diabetes prevalence in a general population from Spain. Environ. Pollut. 235, 948–955. https://doi.org/10.1016/J.ENVPOL.2018.01.008.

Hrdina, J., Banning, A., Kipp, A., Loh, G., Blaut, M., Brigelius-Flohé, R., 2009. The gastrointestinal microbiota affects the selenium status and selenoprotein expression in mice. J. Nutr. Biochem. 20, 638–648. https://doi.org/10.1016/J.JNUTBIO.2008.06.009.

Hu, Z.P., Browne, E.R., Liu, T., Angel, T.E., Ho, P.C., Chan, E.C.Y., 2012. Metabonomic profiling of TASTPM transgenic Alzheimer's disease mouse model. J. Proteome Res. 11, 5903–5913. https://doi.org/10.1021/PR300666P/ASSET/IMAGES/PR300666P.SOCIAL.JPEG_V03.

Huygens, J., Rasschaert, G., Heyndrickx, M., Dewulf, J., Van Coillie, E., Quataert, P., Daeseleire, E., Becue, I., 2022. Impact of fertilization with pig or calf slurry on

antibiotic residues and resistance genes in the soil. Sci. Total Environ. 822 https://doi.org/10.1016/J.SCITOTENV.2022.153518.

Iqbal, J., Zhang, K., Jin, N., Zhao, Y., Liu, Q., Ni, J., Shen, L., 2018. Selenium positively affects the proteome of 3 × Tg-AD mice cortex by altering the expression of various key proteins: unveiling the mechanistic role of selenium in AD prevention. J. Neurosci. Res. 96, 1798–1815. https://doi.org/10.1002/JNR.24309.

Iqubal, A., Ahmed, M., Ahmad, S., Sahoo, C.R., Iqubal, M.K., Haque, S.E., 2020. Environmental neurotoxic pollutants: review, 2020 2733 Environ. Sci. Pollut. Res. 27, 41175–41198. https://doi.org/10.1007/S11356-020-10539-Z.

Ji, F., Luan, H., Huang, Y., Cai, Z., Li, M., 2017. MS-based metabolomics for the investigation of neuro-metabolic changes associated with BDE-47 exposure in C57BL/6 mce, 2017 13 J. Anal. Test. 1, 233–244. https://doi.org/10.1007/S41664-017-0026-4.

Kasaikina, M.V., Kravtsova, M.A., Lee, B.C., Seravalli, J., Peterson, D.A., Walter, J., Legge, R., Benson, A.K., Hatfield, D.L., Gladyshev, V.N., 2011. Dietary selenium affects host selenoproteome expression by influencing the gut microbiota. FASEB J. 25, 2492–2499. https://doi.org/10.1096/FJ.11-181990.

Kim, J., Combs, G.F., 1997. Effects of selenium on colonic fermentation in the rat. Biol. Trace Elem. Res. 56, 215–224. https://doi.org/10.1007/BF02785394.

li Yin, C., gang Lu, R., fang Zhu, J., min Huang, H., Liu, X., feng Li, Q., yi Mo, Y., jia Zhu, H., Chin, B., xia Wu, J., wen Liu, X., Cheng, B., xiang Ruan, J., hong Liang, Y., Song, H., wei Guo, H., heng Su, Z., Zheng, H., 2019. The study of neuroprotective effect of ferulic acid based on cell metabolomics. Eur. J. Pharmacol. 864, 172694 https://doi.org/10.1016/J.EJPHAR.2019.172694.

Lovell, M.A., Xiong, S., Lyubartseva, G., Markesbery, W.R., 2009. Organoselenium (SelPlex diet) decreases amyloid burden and RNA and DNA oxidative damage in APP/PS1 mice. Free Radic. Biol. Med. 46, 1527–1533. https://doi.org/10.1016/J.FREERADBIOMED.2009.03.008.

Mencarelli, C., Martinez-Martinez, P., 2013. Ceramide function in the brain: when a slight tilt is enough. Cell. Mol. Life Sci. 70, 181–203. https://doi.org/10.1007/S00018-012-1038-X.

Pruett, S.T., Bushnev, A., Hagedorn, K., Adiga, M., Haynes, C.A., Sullards, M.C., Liotta, D. C., Merrill, A.H., 2008. Biodiversity of sphingoid bases ('sphingosines') and related amino alcohols. J. Lipid Res. 49, 1621–1639. https://doi.org/10.1194/JLR.R800012-JLR200.

Ramírez-Acosta, S., Huertas-Abril, P.V., Selma-Royo£c, M., Prieto-Álamob, M.J., Colladoc, M.C., Abril, N., García-Barrera, T., 2022b. The role of selenium in shaping mice brain metabolome and selenoproteome through the gut-brain axis by combining metabolomics, metallomics, gene expression and amplicon sequencing. J. Adv. Res. (submitted for publication).

Ramírez-Acosta, S., Selma-Royo, M., Collado, M.C., Navarro-Roldán, F., Abril, N., García-Barrera, T., 2022a. Selenium supplementation influences mice testicular selenoproteins driven by gut microbiota. Sci. Rep. 12, 4218. https://doi.org/10.1038/s41598-022-08121-3.

Rodríguez-Moro, G., Abril, N., Jara-Biedma, R., Ramírez-Acosta, S., Gómez-Ariza, J.L., Garciá-Barrera, T., 2019. Metabolic impairments caused by a 'chemical cocktail' of DDE and selenium in mice using direct infusion triple quadrupole time-of-flight and gas chromatography-mass spectrometry. Chem. Res. Toxicol. 32, 1940–1954. https://doi.org/10.1021/ACS.CHEMRESTOX.9B00102.

Rodríguez-Moro, G., Roldán, F.N., Baya-Arenas, R., Arias-Borrego, A., Callejón-Leblic, B., Gómez-Ariza, J.L., García-Barrera, T., 2020. Metabolic impairments, metal traffic, and dyshomeostasis caused by the antagonistic interaction of cadmium and selenium using organic and inorganic mass spectrometry. Environ. Sci. Pollut. Res. Int 27, 1762–1775. https://doi.org/10.1007/S11356-019-06573-1.

Stadlbauer, V., Engertsberger, L., Komarova, I., Feldbacher, N., Leber, B., Pichler, G., Fink, N., Scarpatetti, M., Schippinger, W., Schmidt, R., Horvath, A., 2020. Dysbiosis, gut barrier dysfunction and inflammation in dementia: a pilot study. BMC Geriatr. 20 https://doi.org/10.1186/S12877-020-01644-2.

Stuve, O., Weideman, R.A., McMahan, D.M., Jacob, D.A., Little, B.B., 2020. Diclofenac reduces the risk of Alzheimer's disease: a pilot analysis of NSAIDs in two US veteran populations. Ther. Adv. Neurol. Disord. 13 https://doi.org/10.1177/1756286420935676.

Sun, D., Yang, N., Zhang, Q., Wang, Z., Luo, G., Pang, J., 2021. The discovery of combined toxicity effects and mechanisms of hexaconazole and arsenic to mice based on untargeted metabolomics. Ecotoxicol. Environ. Saf. 226, 112859 https://doi.org/10.1016/J.ECOENV.2021.112859.

Walter, A., Korth, U., Hilgert, M., Hartmann, J., Weichel, O., Hilgert, M., Fassbender, K., Schmitt, A., Klein, J., 2004. Glycerophosphocholine is elevated in cerebrospinal fluid of Alzheimer patients. Neurobiol. Aging 25, 1299–1303. https://doi.org/10.1016/J.NEUROBIOLAGING.2004.02.016.

Wang, C., Deng, H., Wang, D., Wang, J., Huang, H., Qiu, J., Li, Y., Zou, T., Guo, L., 2021. Changes in metabolomics and lipidomics in brain tissue and their correlations with the gut microbiome after chronic food-derived arsenic exposure in mice. Ecotoxicol. Environ. Saf. 228 https://doi.org/10.1016/J.ECOENV.2021.112935.

Xu, J., ming Xu, H., Peng, Y., Zhao, C., lan Zhao, H., Huang, W., li Huang, H., He, J., lei Du, Y., jian Zhou, Y., lian Zhou, Y., qiang Nie, Y., 2021. The effect of different combinations of antibiotic cocktails on mice and selection of animal models for further microbiota research, 2021 1054 Appl. Microbiol. Biotechnol. 105, 1669–1681. https://doi.org/10.1007/S00253-021-11131-2.

Xu, M.Y., Sun, Y.J., Wang, P., Xu, H.Y., Chen, L.P., Zhu, L., Wu, Y.J., 2015. Metabolomics analysis and biomarker identification for brains of rats exposed subchronically to the mixtures of low-dose cadmium and chlorpyrifos. Chem. Res. Toxicol. 28, 1216–1223. https://doi.org/10.1021/ACS.CHEMRESTOX.5B00054.

Ye, X., Wang, D., Zhu, H., Wang, D., Li, J., Tang, Y., Wu, J., 2021. Gut microbiota changes in patients with major depressive disorder treated with vortioxetine. Front. Psychiatry 12. https://doi.org/10.3389/FPSYT.2021.641491.

Yoshimura, T., Itoh, S., Tsujikawa, K., Yamada, E., Ishii, T., Iemura, O., Kameda, Y., Mimura, T., Kohama, Y., 1998. Effect of 26,26,26,27,27,27-Hexafluoro-1,25-dihydroxyvitamin D3 on the expression of vitamin-D-responsive genes in vitamin-D-deficient mice. Pharmacology 57, 286–294. https://doi.org/10.1159/000028254.

Zarrinpar, A., Chaix, A., Xu, Z.Z., Chang, M.W., Marotz, C.A., Saghatelian, A., Knight, R., Panda, S., 2018. Antibiotic-induced microbiome depletion alters metabolic homeostasis by affecting gut signaling and colonic metabolism. Nat. Commun. 9 https://doi.org/10.1038/S41467-018-05336-9.

Zhai, Q., Cen, S., Li, P., Tian, F., Zhao, J., Zhang, H., Chen, W., 2018. Effects of dietary selenium supplementation on intestinal barrier and immune responses associated with its modulation of Gut Microbiota. Environ. Sci. Technol. Lett. 5, 724–730. https://doi.org/10.1021/ACS.ESTLETT.8B00563/SUPPL_FILE/EZ8B00563_SI_001.PDF.

Zwolak, I., 2020. The role of selenium in arsenic and cadmium toxicity: an updated review of scientific literature. Biol. Trace Elem. Res. 193, 44–63. https://doi.org/10.1007/S12011-019-01691-W.